0090-9556/07/3503-460–468$20.00
DRUG METABOLISM AND DISPOSITION
Vol. 35, No. 3
12401/3181866
DMD 35:460–468, 2007
Printed in U.S.A.
Copyright © 2007 by The American Society for Pharmacology and Experimental Therapeutics

Cross-Species Pharmacokinetic Comparison from Mouse to Man of a Second-Generation Antisense Oligonucleotide, ISIS 301012, Targeting Human Apolipoprotein B-100

Rosie Z. Yu, Tae-Won Kim, An Hong, Tanya A. Watanabe, Hans J. Gaus, and Richard S. Geary

Isis Pharmaceuticals, Carlsbad, California

Received August 8, 2006; accepted December 12, 2006

ABSTRACT:

The pharmacokinetics of a 2′-*O*-(2-methoxyethyl)-modified oligonucleotide, ISIS 301012 [targeting human apolipoprotein B-100 (apoB-100)], was characterized in mouse, rat, monkey, and human. Plasma pharmacokinetics following parental administration was similar across species, exhibiting a rapid distribution phase with $t_{1/2\alpha}$ of several hours and a prolonged elimination phase with $t_{1/2\beta}$ of days. The prolonged elimination phase represents equilibrium between tissues and circulating drug due to slow elimination from tissues. Absorption was nearly complete following s.c. injection, with bioavailability ranging from 80 to 100% in monkeys. Plasma clearance scaled well across species as a function of body weight alone, and this correlation was improved when corrected for plasma protein binding. In all of the animal models studied, the highest tissue concentrations of ISIS 301012 were observed in kidney and liver. Urinary excretion was less than 3% in monkeys and human in the first 24 h. ISIS 301012 is highly bound to plasma proteins, probably preventing rapid removal by renal filtration. However, following 25 mg/kg s.c. administration in mouse and 5-mg/kg i.v. bolus administration in rat, plasma concentrations of ISIS 301012 exceeded their respective protein binding capacity. Thus, urinary excretion increased to 16% or greater within the first 24 h. Albeit slow, urinary excretion of ISIS 301012 and its shortened metabolites is the ultimate elimination pathway of this compound, as demonstrated by 32% of dose recovered in total excreta by 14 days in a rat mass balance study. The pharmacokinetics of ISIS 301012 in human is predictable from the pharmacokinetics measured in animals. The pharmacokinetic properties of ISIS 301012 provide guidance for clinical development and support infrequent dose administration.

Downloaded from dmd.aspetjournals.org at ASPET Journals on March 5, 2016

There have been continued advancements toward identification of chemical modifications that improve upon the pharmacokinetic and pharmacodynamic properties of antisense oligonucleotides (ASOs) over the years (Wagner, 1994; Altmann et al., 1996; Lima et al., 1997; Manoharan, 1999). Among the majority of these modified phosphorothioate (PS) oligonucleotides, the 2′-*O*-methoxyethyl (2′-MOE)-modified PS oligodeoxynucleotides have consistently demonstrated greater biological stability, higher binding affinity to the target mRNA while maintaining RNase H activity by using a chimeric design strategy (Manoharan, 1999), and decreasing general nonhybridization toxicities (McKay et al., 1999; Henry et al., 2001). These modifications are commonly known as second-generation ASOs. Several MOE-modified oligonucleotides are in clinical development, including ISIS 104838 for the treatment of rheumatoid arthritis (Sewell et al., 2002; Wei et al., 2003), ISIS 113715 for the treatment of diabetes (Kjems, 2005), OGX-011 for the treatment of prostate cancer (Chi et al., 2005), and LY2181308 for the treatment of solid tumors (Jones and Schreiber, 2005). The MOE modification has led to the development of potent, pharmacologically active, specific antisense oligonucleotides, one of which is ISIS 301012.

ISIS 301012 is a 20-base partially 2′-MOE modified ASO, also referred to as a MOE gapmer, where the term "gap" refers to the 10 2′-deoxyribonucleosides that are necessary to support enzymatic cleavage of the mRNA (the chimeric design). ISIS 301012 binds to the coding region of the human apoB-100 mRNA (position 3249–3269 base pair) by Watson and Crick base pairing. The hybridization of ISIS 301012 to apoB-100 mRNA results in RNase H-mediated degradation of the cognate mRNA, thereby inhibiting the translation of the apoB protein. ApoB-100 is the principal apolipoprotein of very low-density lipoprotein cholesterol, intermediate-density lipoprotein cholesterol, and low-density lipoprotein cholesterol (Das et al., 1988; Davidson and Shelness, 2000; Marsh et al., 2002). Thus, apoB-100 inhibition is a promising target for the development of new treatment options to lower low-density lipoprotein cholesterol. ISIS 301012 represents the first antisense compound of the lipid-lowering class to be dosed in human (Bradley et al., 2005; Crooke et al., 2005; Kastelein et al., 2006). The in vitro pharmacological activity of ISIS 301012

Article, publication date, and citation information can be found at http://dmd.aspetjournals.org.
doi:10.1124/dmd.106.012401.

ABBREVIATIONS: ASO, antisense oligonucleotide; PS, phosphorothioate; MOE, *O*-methoxyethyl; ApoB-100, apolipoprotein B-100; HPLC, high-performance liquid chromatography; MS, mass spectrometry; QWBA, quantitative whole-body autoradioluminography; MD, multiple dose; ELISA, enzyme-linked immunosorbent assay; ES, electrospray; CGE, capillary gel electrophoresis; IP, ion pairing; *F*, bioavailability; CL_p, plasma clearance; CL_u, unbound intrinsic clearance; AUC, area under the curve.

had been demonstrated in several human cell lines (HepG2 and Hep3B) and primary human hepatocytes, where IC_{50} values were in the range of 10 to 50 nM for target mRNA reduction.

As expected, there has been significantly more information published regarding the pharmacokinetic properties of first-generation PS oligodeoxynucleotides since they commenced in the early 1990s (Cossum et al., 1993; Agrawal et al., 1995; Geary et al., 1997b; Leeds et al., 1997; Grindel et al., 1998; Yu et al., 2001a,b) (to cite just a few). Second-generation ASOs are relatively early in their development, and pharmacokinetic data are less plentiful (Geary et al., 2001a, 2003; Sewell et al., 2002). The pharmacokinetics of ISIS 301012 has been characterized in mice, rats, and monkeys during preclinical development. In addition, selected pharmacokinetic data in human from a phase I healthy volunteer study is also included in this article. A compilation of the results of these important studies is described here, representing a complete preclinical pharmacokinetic profile for a 2′-*O*-(2-methoxyethyl) partially modified antisense phosphorothioate oligonucleotide. Furthermore, the pharmacokinetic analyses used in this study provide guidance for the development of future oligonucleotide in this chemical class.

Materials and Methods

Test Compound. ISIS 301012 is a 20-base phosphorothioate oligonucleotide with a total of 10 2′-*O*-methoxyethyl-modified ribofuranosyl nucleotides, five on each end of the oligonucleotide (Fig. 1). Full-length purity of the test compound [as determined by liquid chromatography-mass spectrometry (MS)] was 92.8% with 0.5% of the impurities associated with N-1 (deletion sequence). Dosing was performed based on the quantity of full-length 20-mer oligonucleotide.

Radiolabeled ISIS 301012 was mixed together with nonradioactive ISIS 301012 for radiolabel disposition and mass balance studies in rat. The radiolabel was tritium incorporated into the nonexchangeable 5-carbon position of the ribose sugar of one of the deoxy-thymidine nucleotides in the gap portion of the oligonucleotide (Fig. 1). The radiolabel purity of [^{3}H]ISIS 301012 was >99% by HPLC. The specific activity of [^{3}H]ISIS 301012 ranged from 20 to 100 μCi/mg.

Test Systems. Male and female CD-1 mice [Crl:CD-1 (ICR) BR; Charles River Laboratories, Inc., Wilmington, MA], male Sprague-Dawley rats [Crl: CD(SD)IGS BR; Charles River Canada, Montreal, QC, Canada], and male and female cynomolgus monkeys, *Macaca fascicularis* (Sierra Biomedical Animal Colony, Sparks, NV) received either intravenous (i.v.) infusion or subcutaneous (s.c.) injection of ISIS 301012 at doses ranging from 2 to 50 mg/kg. All animal studies were conducted using protocols and methods approved by the Institutional Animal Care and Use Committee and carried out in accordance with the *Guide for the Care and Use of Laboratory Animals* adopted and promulgated by the United States National Institutes of Health (Bethesda, MD).

Mouse. Male and female CD-1 mice were administered ISIS 301012 doses of 2, 5, 25, or 50 mg/kg via s.c. injections every other day for four doses (loading regimen), followed by every 4th day dosing for the duration of a 13-week toxicology study. Drug concentrations were measured in plasma for satellite pharmacokinetic animals receiving the 5- and 25-mg/kg doses. Blood samples were collected for ISIS 301012 quantitation in plasma by cardiac puncture at sacrifice in tubes containing EDTA at 15, 30, and 60 min and 2, 4, 8, 24, and 48 h after the first dose and the 10th dose (day 31) (three male mice per time point). Urine collection over a 48-h period at 24-h interval was done immediately after the first dose at the 5- and 25-mg/kg dose levels. Drug concentrations were measured in various types of tissues (including liver and kidney) collected at sacrifice approximately 48 h after the last dose (day 93) for all dose groups (2–50 mg/kg). In addition, concentrations of ISIS 301012 were also measured in tissues of mice receiving the 5- and 50-mg/kg dose sacrificed 91 days after completion of 3-month treatment regimen (on day 181) to assess clearance during a 3-month recovery phase.

Rat. Single dose i.v. injections of 5 and 24 mg/kg [^{3}H]ISIS 301012 were administered to male Sprague-Dawley rats. The dose volume was 5 and 6 ml/kg, and the total amount of radioactivity administered was 120 and 1009 μCi/kg, respectively. Before dosing, each animal selected for blood collection had a jugular cannula implanted. After a single i.v. dose of 5 mg/kg [^{3}H]ISIS 301012, whole blood was collected in tubes containing EDTA at 2, 30, and 60 min and at 2, 4, 8, 12, 16, 24 36, 48, 168, 336, and 672 h postdose from three animals per time point. Urinary excretion after the 5-mg/kg dose was assessed at various intervals over a 336-h period. Mass balance recovery of radiolabel in urine, feces, tissue, carcass, and cage wash was assessed at 24 and 336 h (or 1 and 14 day after single-dose administration, 5 mg/kg). Half-lives of total radiolabel were calculated in multiple tissues at a dose of 5 mg/kg (120 μCi/kg) over the 28 days after radiolabeled ISIS 301012 administration. Quantitative whole-body autoradioluminography (QWBA) was performed for rats that received 24 mg/kg (1009 μCi/kg) dose at 48 h.

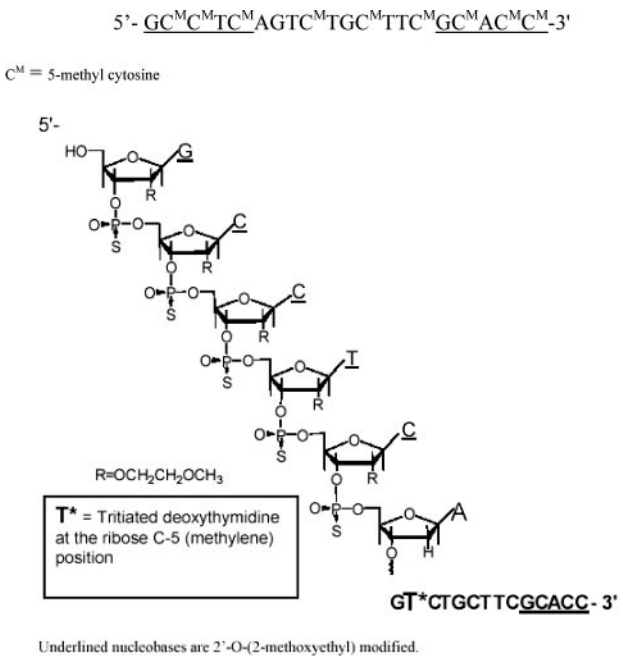

FIG. 1. Sequence of ISIS 301012 fully thioated 20-mer. Boldface and underlined nucleotides are 2′-*O*-(2-methoxyethyl)-modified. Center gap, deoxynucleotide (DNA). Stable tritium ^{3}H label incorporated on 5′ carbon of an unmodified thymidine residue in ISIS 301012 oligonucleotide.

Monkey. Single- and multiple-dose pharmacokinetic studies were conducted in male and female cynomolgus monkeys. Dose levels for ISIS 301012 included 2, 4, and 12 mg/kg administered via 1-h i.v. infusion and 20 mg/kg administered by s.c. injection. Doses were administered as every other day for four doses (1 week), followed by dosing once every 4th day for the remainder of a 13-week dosing period. On days 7, 27, and 87 (after the 4th, 10th, and 24th doses, respectively), blood was collected for quantitation of ISIS 301012 in plasma by peripheral venipuncture into EDTA-containing Vacutainers just before dosing and 1, 2, 4, 8, 24, and 48 h after i.v. infusion or s.c. injection. After the fourth dose of 4 mg/kg ISIS 301012, additional plasma samples were taken 3, 4, 8, 16, 32, and 48 days postdose to assess the terminal elimination half-life in plasma. Urine was collected over a 48-h period at 24-h interval immediately after the first dose administration from all dose groups. Drug concentrations were measured in various types of tissues (including liver and kidney) from all dose groups at scheduled terminations (day 33 and day 89 sacrifice) and recovery period (day 181 sacrifice). Accumulation during the loading phase and tissue half-lives were determined in monkeys receiving the 4-mg/kg dose euthanized (one monkey per sex per time point) after a single dose (48 h after first dose) or after four loading doses (48 h and 4, 8, 16, 32, and 48 days after the fourth dose).

Human. In a phase I clinical study, human healthy volunteers received ISIS 301012 after 2-h i.v. infusion and s.c. injections at doses that ranged from 50 to 400 mg (Kastelein et al., 2006). In brief, 29 healthy volunteer subjects in this study received either 50 mg ($n = 8$), 100 mg ($n = 8$), 200 mg ($n = 9$), and 400 mg ($n = 4$) per dose day; seven subjects received placebo. The multiple-dose (MD) period consisted of three i.v. infusions (on MD1, MD3, and MD5) over

Downloaded from dmd.aspetjournals.org at ASPET Journals on March 5, 2016

2 h every other day during the 1st week, followed by once weekly s.c. injections for 3 weeks (total of six doses over 22 days) (on MD8, MD15, and MD22). Intensive pharmacokinetic blood sampling occurred for 24 h after the first i.v. dose (at 0, 0.5, 1, 2, 2.25, 2.5, 3, 4, 6, 8, and 24 h) and again after the last s.c. dose (MD22) (at 0, 0.5, 1,1.5, 2, 3, 4, 6, 8, 12, and 24 h). In addition, trough blood samples for determination of elimination half-life were collected the post-treatment follow-up period, at 3, 17, 33, 47, 61, 75, and 89 days after the last s.c. dose. Samples were collected in EDTA tubes, and plasma was harvested. Urine for pharmacokinetics was collected for the first 24 h after the first i.v. dose and last s.c. dose. Selected pharmacokinetic data from the phase I study have been compared with preclinical data, and findings are summarized.

Analytical Methods. *Hybridization enzyme-linked immunosorbent assay.* Plasma samples were analyzed using a quantitative, sensitive hybridization ELISA method, which is a variation on the method reported previously (Yu et al., 2002). The assay was validated for precision, accuracy, selectivity, sensitivity, and stability of ISIS 301012 quantitation before analysis of mouse, monkey, and human plasma samples. Plasma sample analyses were conducted at PPD Development (Richmond, VA) and were performed based on the principles and requirements described in 21 CFR part 58. The assay conducted with synthesized putative shortened oligonucleotide metabolite standards showed no measurable cross-reactivity, confirming the assays specificity for the parent oligonucleotide. The lower limit of quantitation was determined to be 1.52 ng/ml. This assay was also used to quantitate ISIS 301012 concentrations in rat plasma after a single i.v. dose of 5 mg/kg [^{3}H]ISIS 301012.

Protein binding assay. An ultrafiltration method (Watanabe et al., 2006) was used to assess whole-plasma protein binding characteristics of ISIS 301012. In brief, Millipore Corporation (Bedford, MA) Ultrafree-MC filters (mol. wt. cut-off of 30 kDa) were used. ISIS 301012 was labeled with ^{32}P before addition of the oligonucleotide to plasma (Sambrook et al., 1982). Whole-plasma binding of four species (mouse, rat, monkey, and human) was evaluated over the plasma concentration range of 7.6 to 152 μg/ml. In addition, protein binding in human plasma with selected ISIS 301012 metabolites (N-1 and N-10 or 19-mer and 10-mer) was conducted over the concentration range of 0.1 to 50 μM ISIS 301012 (equivalent to approximately 0.76 to 380 μg/ml ISIS 301012). Due to differences in the molecular weight of the ISIS 301012 metabolites, the plasma concentrations were prepared as micromolar-equivalent concentrations in comparison of length-based plasma protein binding. Five replicates were used to calculate average radiolabel counts and standard deviations.

Capillary gel electrophoresis. Validated CGE methods were used to measure unlabeled drug concentrations in mouse and monkey urine and tissues as well as human urine. The methods for ISIS 301012 are modifications of previously published methods (Leeds et al., 1996; Geary et al., 1999). An internal standard (ISIS 13866, a 27-mer 2′-*O*-methoxyethyl-modified phosphorothioate oligonucleotide) was added before extraction. Tissue sample analyses were conducted at Southwest Bio-Labs, Inc. (Las Cruces, NM), whereas urine samples were analyzed at Isis Pharmaceuticals (Carlsbad, CA) Tissue and urine sample analyses were performed based on the principles and requirements described in 21 CFR part 58. For urine and tissues, the limits of quantitation were 0.076 μg/ml and 1.52 μg/g, respectively.

Radiometric analysis (liquid scintillation counting). Radioactivity in rat samples was quantitated by liquid scintillation counting using a Beckman 6001C counter (Beckman Coulter., Fullerton, CA). Urine and plasma samples were directly mixed with Ultima Gold LSC cocktail (PerkinElmer Life and Analytical Sciences, Boston, MA). For solubilized tissue samples, Hionic Fluor LSC cocktail was used (PerkinElmer Life and Analytical Sciences). Oxygen combustion of feces and bone was carried out using a model 307 tissue oxidizer (PerkinElmer Life and Analytical Sciences). Ultima Gold cocktail was used to trap the ^3H_2O generated from each sample. The scintillation counter was operated in the background subtract mode and samples were counted for 5 min or to a 2-σ error of 0.1%, whichever occurred first. All counts were converted to absolute radioactivity (disintegration/minute) by automatic quench correction based on the shift of the spectrum for the external standard.

Quantitative whole-body autoradioluminography. Rats were sacrificed 48 h after the 24-mg/kg (200-μCi) i.v. dose administration, and animal carcasses were deep-frozen in a mixture of hexane and dry ice. Each animal specimen was then embedded lying on its right side in a 2% carboxymethylcellulose medium using a freezing frame to collect sagittal whole-body sections. Each animal specimen block was sectioned using the CM 3600 cryomicrotome (Leica Microsystems, Inc., Deerfield, IL). Sections (30 μm) were collected and were frozen dry in the microtome cryocabinet for at least 16 h. Sections were then exposed to ^{3}H imaging plate for a predetermined time in a lead box and refrigerated at ≈4°C to minimize background radiation artifacts. After exposure, the imaging plate was read by the Fuji BAS-2500 scanner and its Fuji Image Reader software version 1.1 (Fujifilm, Tokyo, Japan). From the autoradioluminograms obtained, the amount of radioactivity in tissues was quantified from each animal with reference to calibration curve generated by known [^{3}H]glucose standard radioactivity concentrations using the Fuji Image Gauge Analysis software (Fujifilm).

HPLC-ES/MS metabolite identification of ISIS 301012 and metabolites. Selected urine samples from monkey and human were analyzed for metabolite identification purposes by ion pairing (IP) HPLC-ES/MS. Separation was accomplished using a 1100 HPLC-MS system (Agilent Technologies, Wilmington, DE) consisting of a quaternary pump, variable wavelength UV-detector, a column oven, an autosampler, and a single quadrupole mass spectrometer (Agilent Technologies). Typically, 500 μl of each sample was extracted using a two-step solid phase extraction in series (strong anion exchange followed by reverse-phase C18) method, reconstituted in mobile phase, and injected directly on a YMC AQ C18 column (150 × 1.0 mm; 3-μm particles; 200-Å pore size; Waters, Milford, MA). The column was maintained at 35°C, and the flow rate on the column was 0.1 ml/min. The column was equilibrated with 35% acetonitrile in 5 mM tributylammonium acetate, pH 7.0. A gradient from 35 to 75% acetonitrile over 27 min was used to separately elute ISIS 301012 and shortened oligonucleotide metabolites. Absorbance was measured at 260 nm. Under these conditions, oligonucleotides differing by a single nucleotide could be resolved.

Mass measurements were made online using a single quadrupole mass spectrometer (Agilent Technologies). From 4 to 30 min, the mass spectrometer was set to scan a *m*/*z* window of 800 to 1920. Mass spectra were obtained using a spray voltage of 4 kV, a sheath gas flow of 35 pounds per square inch gauge, a drying gas flow rate of 12 l/min at 335°C, and a capillary voltage of −150 V. Chromatograms were analyzed using ChemStation software (Agilent Technologies). Potential metabolite peaks were identified either from the total ion current trace or from the UV trace. Each peak was manually averaged for its *m*/*z* value, and the results were compared with a table containing the calculated *m*/*z* values of expected metabolites.

Pharmacokinetic analysis. Both compartmental and noncompartmental analysis methods were used for pharmacokinetic characterization of the plasma concentration data (WinNonlin 4.0; Pharsight, Mountain View, CA). Plasma bioavailability (*F*) following subcutaneous administration relative to i.v. administration in monkey and human was calculated by the ratio of the dose-normalized plasma AUCs.

Cross-species regression using allometry was performed by linear regression of plasma clearance (CL_p) versus body weight (W). The equation used to relate the pharmacokinetic parameters (*Y*) to body weight (W) was as follows: $Y = aW^b$.

In addition, correction on clearance was made for plasma protein binding, where the unbound intrinsic clearance (CL_u) was calculated by $CL_u = CL_p/f_u$, where f_u is unbound fraction of ISIS 301012 in plasma. Thus, a log-log regression of a pharmacokinetic parameter Y (i.e., CL_p or CL_u) versus W will yield a *y*-intercept value of *a* and a slope of *b*. The sign and magnitude of the exponent (*b*) indicates how the physiological variable is changing as a function of W (Boxenbaum, 1982). Clearance estimates were adjusted by mean body weight for mouse, rat, monkey, and human.

First-order elimination rates for ISIS 301012 in tissue were calculated using noncompartmental nonlinear regression of the decay curves for the respective tissues. Half-life was calculated by dividing 0.693 by the first-order elimination rate.

Results

Plasma Pharmacokinetics. The plasma concentration-time profile decreased rapidly in a polyphasic manner for mouse, rat, monkey, and human after s.c., i.v. bolus and 1- or 2-h i.v. administration (Table 1; Fig. 2, A and B). The initial $t_{1/2\alpha}$ after i.v. bolus administration was

Downloaded from dmd.aspetjournals.org at ASPET Journals on March 5, 2016

TABLE 1

Plasma pharmacokinetic parameter estimates for ISIS 301012 compared across species

Standard deviation of the estimates is shown in parentheses.

Parameter	Mouse	Rat[a]	Monkey	Human
Dose and route	5 mg/kg s.c.	5 mg/kg i.v. bolus	4 mg/kg 1-h i.v. infusion	200 mg 2-h i.v. infusion
C_{max} (μg/ml)	3.8 (0.57)	73.9 (2.4)	39.8 (6.7)	21.5 (4.2)
T_{max} (h)	0.5	2 min	1 (0)	1.98 (0.21)
AUC (μg · h/ml)	7.41	27.7	82.0 (19.1)	68.2 (13.5)
$t_{1/2\alpha}$ (h)	0.33	0.39	0.68 (0.19)	1.26 (0.16)
$t_{1/2\beta}$ (day)	NM	4.7[b]	16[c]	31.1 (11.4)[d]
CL_p (ml/h/kg)[e]	674	181	51.1 (11.1)	40.9 (5.12)
V_{ss} (l/kg)[e]	NM	1.0	7.7[c]	48.3 (14.7)[d]

[a] ISIS 301012 concentrations were measured using cold assay, hybridization ELISA method.
[b] Plasma concentration-time profile seemed triphasic, with a half-life of 2.9 h in the second phase; thus, this half-life represents the terminal half-life. Additionally, the terminal half-life may be underestimated because of limited time points.
[c] $n = 2$.
[d] Determined following s.c. administration.
[e] CLp/F and V_z/F reported for s.c. dosing.

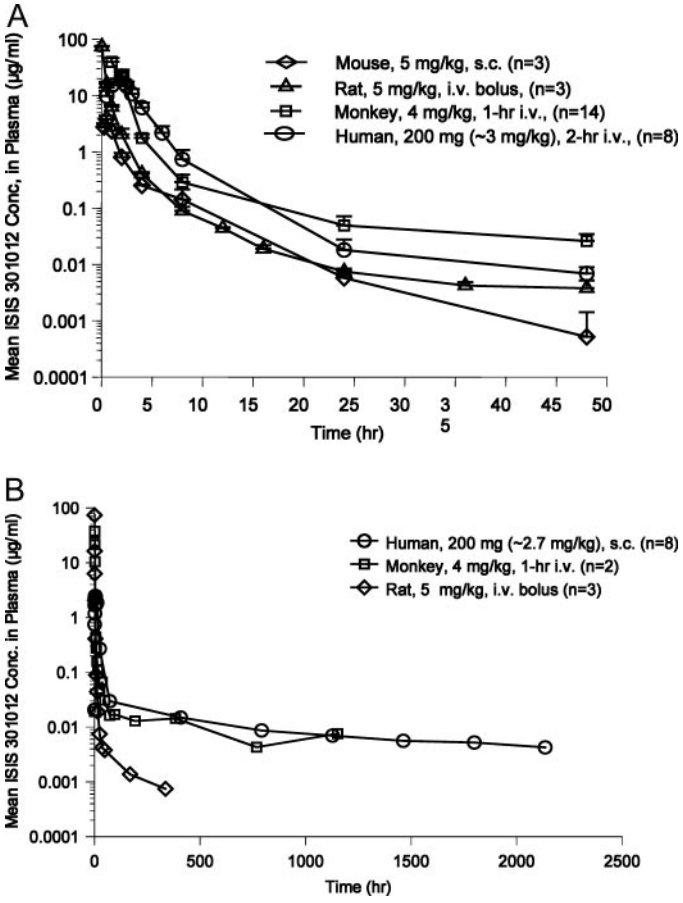

FIG. 2. Polyphasic pharmacokinetic profiles of ISIS 301012 in mouse, rat, monkey, and human during distribution (A) and in monkey and human during elimination phase (B). ISIS 301012 concentrations in plasma were measured using a hybridization ELISA method in mouse, rat, monkey, and human.

relatively fast, generally ≤1 h. In monkeys, mean absolute *F* after s.c. dosing was 82.8% (Table 2), which would seem to indicate nearly complete systemic absorption by this route of administration. Comparison of tissue levels after s.c. dosing indicates essentially equivalent levels of oligonucleotide in tissues of distribution, again indicating essentially complete absorption by the route of administration.

Use of an ultrasensitive hybridization ELISA method provided characterization of a slow-terminal elimination phase in rat, monkey, and human (Fig. 2B), with a half-life that ranged from 4.7 to 31 days (Table 1). The ISIS 301012 concentration decline in plasma slowed

TABLE 2

Subcutaneous administration of ISIS 301012 to monkeys resulted in essentially complete bioavailability measured by both plasma AUC (day 7) and tissue concentrations of ISIS 301012 measured 48 h after the last dose administered over a 13-week period

Parameter	12 mg/kg i.v.	20 mg/kg s.c.	*F* (%)[a]
Plasma AUC (μg · h/ml)	310	428	82.8
Kidney cortex (μg/g)	1304	1593	73.3
Kidney medulla (μg/g)	684	1221	107
Liver (μg/g)	584	1129	116
Lung (μg/g)	26.9	61.6	137
Mesenteric lymph (μg/g)	459	767	100
Heart (μg/g)	46.9	93.2	119
Bone marrow (μg/g)	104	217	125

[a] $F\ (\%) = \{(C_{s.c.}/\text{Dose}_{s.c.})/(C_{i.v.}/\text{Dose}_{i.v.})\} \times 100$, where *C* represents the respective tissue concentration of ISIS 301012 on day 89.

dramatically after nearly complete distribution, which is reflected by a 2 to 4 log decline of ISIS 301012 concentrations in plasma over a period of approximately 24 h. The apparent terminal elimination rate in monkey plasma, with a half-life of approximately 16 days, was consistent with the slow elimination of ISIS 301012 from monkey tissues; thus, it seems to reflect equilibrium with oligonucleotide in tissue. The terminal elimination phase observed in human was similar to that observed in monkey (Fig. 2B) at a similar milligram per kilogram dose. Consistent with extensive distribution and the long elimination half-lives, the volume of distribution at steady state was large. For example, the volume of distribution was 7.7 l/kg in the monkey and was 48.3 l/kg in human, consistent with extensive distribution of ISIS 301012.

Allometric comparison of clearance estimated at doses ranging from 4 to 5 mg/kg across all species from mouse to man shows a linear relationship ($b = 0.65$; $r^2 = 0.95$) based on body weight alone (Fig. 3A). This correlation improved when clearance was corrected by plasma protein binding (CL_u) ($b = 0.75$; $r^2 = 0.97$) (Fig. 3B).

Protein Binding. The percentage of ISIS 301012 bound to plasma proteins was ≥85% across the concentration range tested (7.6–152 μg/ml) in all species (Fig. 4a). The plasma binding extent was highest in human and lowest in mouse among the species studied. The lower plasma protein binding extent in mouse could partially explain its more rapid clearance. Therefore, allometric scaling of clearance across species corrected by plasma protein binding improved the correlation (Fig. 3B). Plasma protein binding seems to be length-dependent, because shorter metabolites (N-1 and N-10) were less plasma protein bound, with the free fraction of N-10 increased 2- to 3-fold compared with ISIS 301012 in human plasma (Fig. 4B).

Tissue Distribution and Pharmacokinetics. Tissue distribution in

Downloaded from dmd.aspetjournals.org at ASPET Journals on March 5, 2016

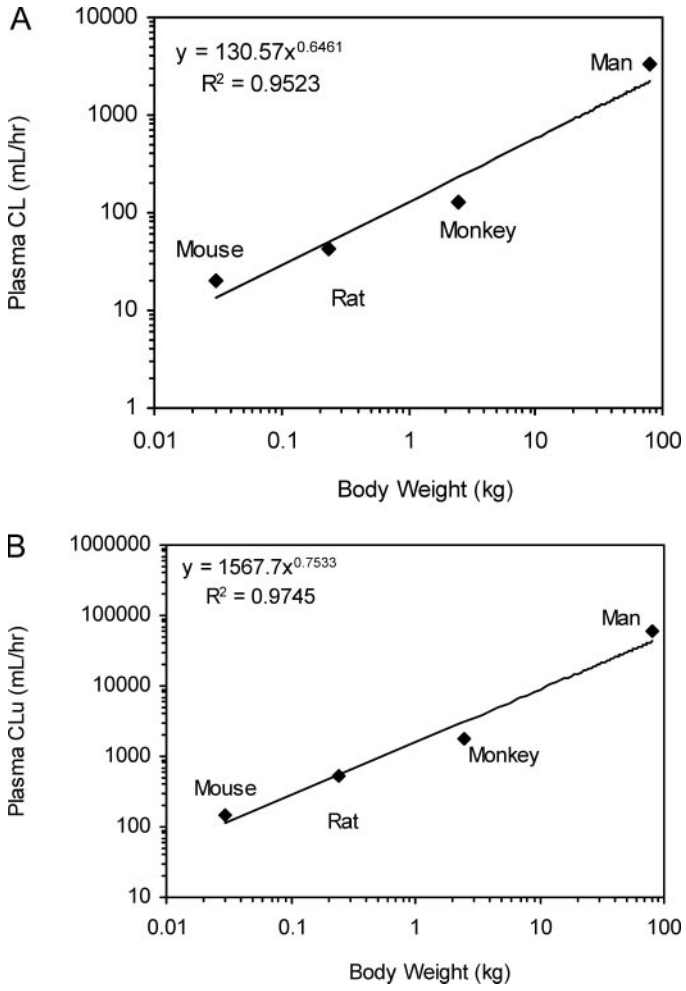

FIG. 3. Allometric relationship across species of clearance with body weight (a) or CL_u with body weight (b). Doses ranged from 4 to 5 mg/kg.

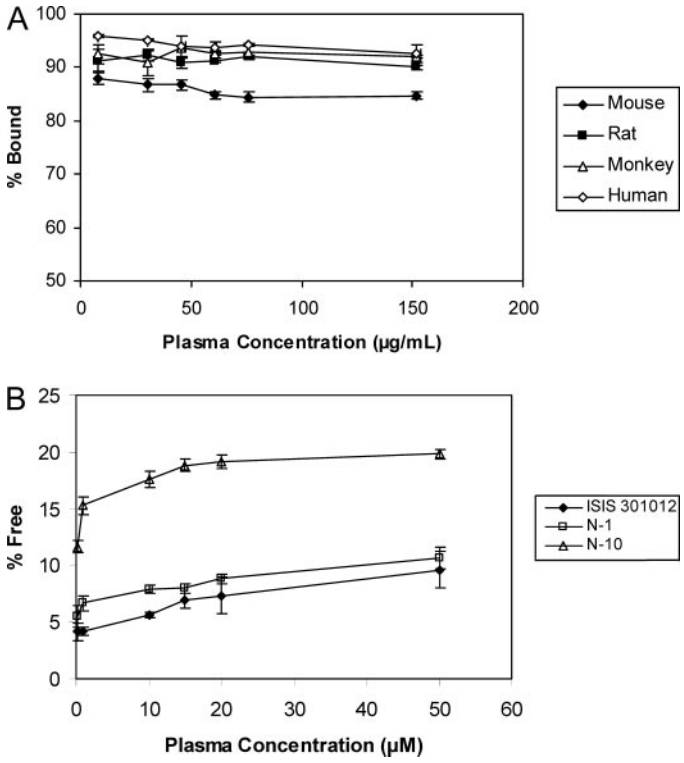

FIG. 4. Bound fraction of [^{32}P]ISIS 301012 to whole-plasma protein across species (A) and free fraction of ^{32}P-labeled ISIS 301012 as well as metabolites in whole-human plasma protein (B) as a function of concentration added. Each point represents the mean of five measurements; error bar represents standard deviation.

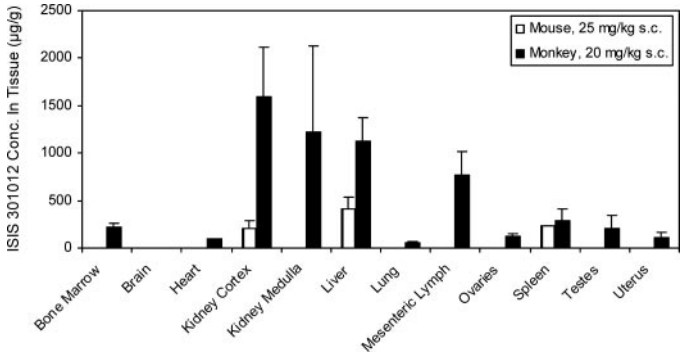

FIG. 5. Comparison of ISIS 301012 concentrations in tissues taken 48 h after the last dose administered over 3 months to CD-1 mice and cynomolgus monkeys. Each bar represents the average of three to six measurements (CGE-UV). Error bars are mean ± S.D.

mouse, rat, and monkey (Figs. 5 and 6) was similar, where the highest concentrations of oligonucleotides were found in kidney and liver. Although highest concentrations were seen in liver of mice, the highest concentrations in rats and monkeys were observed in kidney. Slightly lower concentrations were detected in lymph nodes, spleen, and bone marrow. The concentrations found in heart, lung, ovaries, uterus, and testes were much lower, with no distribution to brain. Tissue concentrations of ISIS 301012 were generally higher in monkeys than in mice at comparable dose levels (Fig. 5).

After a 20 mg/kg s.c. injection of ISIS 301012 in monkeys, the bioavailability in tissue exposure was nearly 100% (Table 2). The high tissue concentrations suggests that there was complete absorption from the subcutaneous injection site with oligonucleotide reaching tissues in a pattern and at levels similar to intravenous administration, consistent with plasma pharmacokinetics.

Clearance of ISIS 301012 from tissues is dependent on metabolism and was slow compared with the initial plasma clearance. Tissue elimination half-lives for ISIS 301012 were similar across species and were ≥13 days in rats compared with 18 to 35 days in monkeys, depending on tissue (Table 3). In addition, tissue clearance was monitored in mice and monkeys during the recovery phase of the toxicology studies. Concentrations of ISIS 301012 decreased approximately 2- to 44-fold in mouse tissues and 4- to 6-fold in monkey tissues after 3 months of treatment-free recovery period (day 181) (internal report).

Excretion. Urinary excretion of total oligonucleotide, within the first 24 h after a single dose, accounted for only a small percentage of the administered dose in mouse, rat, and monkey (Table 4). In general, the percentage of urinary excretion seemed to be dose-dependent as studied in mouse, monkey, and human. Urinary excretion in mouse increased with increasing dose, with approximately 1.05 and 23.7% of the dose recovered in urine 24 h after a single dose of 5 and 25 mg/kg, respectively. The dose dependence of ISIS 301012 excretion in mouse is most probably due to increasing concentrations of unbound drug at higher plasma drug concentrations, which was reflected in its lower plasma protein binding extent. Consistent with this but to a lesser extent, the dose-dependent urinary excretion of ISIS 301012 was observed in monkey and human. The dose-dependent differences are less in monkey and human, probably due to greater plasma protein binding extent (Fig. 4B) compared with mouse. The majority of

Downloaded from dmd.aspetjournals.org at ASPET Journals on March 5, 2016

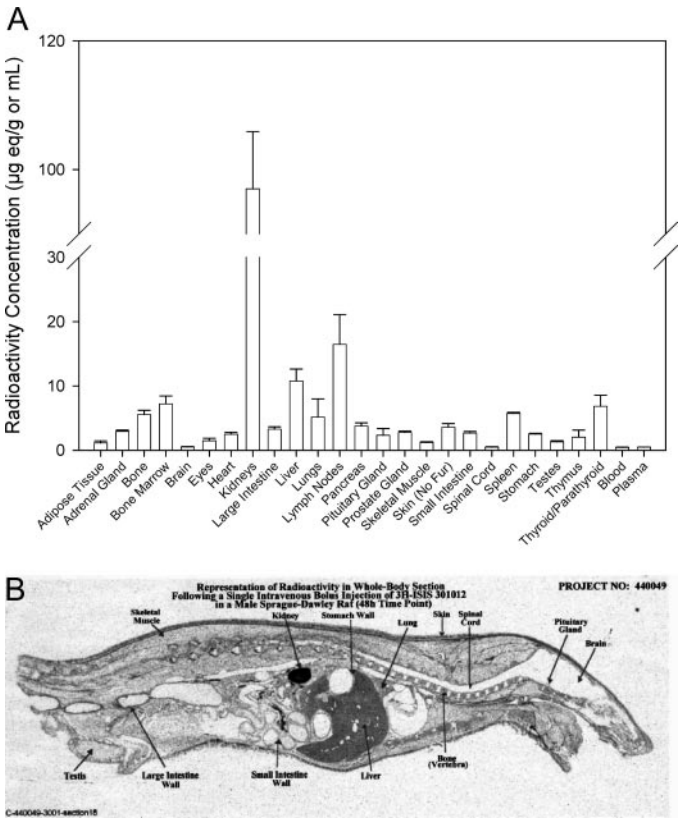

FIG. 6. Distribution of radiolabel associated with [^{3}H]ISIS 301012 presented by quantitation of radio label by liquid scintillation (microgram-equivalents per milliliter of blood or plasma and microgram-equivalents per gram of tissue) in rat 48 h after single i.v. administration at a dose of 5 mg/kg [^{3}H]ISIS 301012 ($n = 3$) (A) and by QWBA in male rat, 48 h after a single intravenous bolus dose of 24 mg/kg [^{3}H]ISIS 301012 (B). The darkness of the gray scale on the QWBA figure represents the level of radioactivity, with white being the lowest and black being the highest level.

TABLE 3

Estimated elimination half-life (in days) of ISIS 301012 from selected tissues in rat and monkey

Tissue	Rat[a]	Monkey
Dose	5 mg/kg [^{3}H]ISIS 301012	4 mg/kg ISIS 301012
Kidney[b]	>28	7[c], 33
Liver	13	34
Mesenteric lymph node	>28	35
Heart	>28	18

NM, not measured.

[a] Value is reported as >28 days because the sampling times were collected for 28 days (less than one half-life) and were insufficient to determine elimination half-life. In addition, half-life was estimated from total radioactivity.

[b] Whole kidney in rat; kidney cortex in monkey.

[c] Concentration-time profile seems biphasic with a 7-day initial half-life and apparent terminal elimination half-life of 33 days.

urinary excretion occurred within the first 24 h after dose administration, and excretion decreased dramatically in the next 24-h period (24- to 48-h collection) (data not shown). This biphasic urinary excretion represents a greater extent of excretion when plasma concentrations are higher (early in the plasma profile), again probably associated with higher levels of unbound drug.

After i.v. bolus administration of 5 mg/kg ^{3}H-radiolabeled ISIS 301012 in rats, the percentage of total radiolabel dose excreted in urine was approximately 16% over the first 24 h (Table 4). Albeit slow, urinary excretion is a continuous process, as presented in Fig. 7. Approximately 26% of the ISIS 301012-associated radiolabel in rats was excreted by 2 weeks after a single dose. Fecal excretion accounted for less than 5% of the administered dose over the same 2-week period after a single i.v. dose in rats. Urinary and fecal excretion are minor contributors to initial plasma clearance of drug with less than 20% excreted in urine and 5% in feces in 24 h. However, urinary excretion was the major route of whole-body clearance with continuous albeit slow excretion of parent oligonucleotide and nuclease-generated metabolites. The mean mass balance of radioactivity recovered was approximately 83% of the administered dose at the 24- and 336-h time points. The majority of radioactivity (approximately 51%) was associated with the tissues (including carcass) and approximately 32% was associated with total excreta and the gastrointestinal tract contents (26% in urine, 4.2% in feces, 0.99% in cage wash, and 0.44% in the gastrointestinal tract contents) after 2 weeks (336 h). These findings seemed to be consistent with relatively rapid and almost complete distribution of [^{3}H]ISIS 301012-related radioactive residues from the blood to tissues after intravenous administration, followed by relatively slow clearance of the radiolabeled species from tissues into the excreta (mainly urine).

In monkey and human, urinary excretion of total oligonucleotide within the first 24 h, accounted for only a small percentage of the administered dose (mean excretion less than 4% of administered dose) after a single dose up to 12 mg/kg in monkey and 200 mg in human given by 1- or 2-h infusion (Table 4). In addition to parent compound, putative oligonucleotide metabolites consistent with mainly endonuclease-mediated cleavage were evident in most of the collected urine samples in monkey and human (Fig. 8). However, ISIS 301012 was typically the most abundant species of oligonucleotides and generally accounted for >60% of the total oligonucleotide in the urine samples.

Urinary Metabolite Identification. Numerous ISIS 301012 metabolites were detected in urine collected 0 to 24 h after dose administration in monkey and human. These metabolites were characterized using a sensitive IP-HPLC-ES/MS method and confirmed the identity of these shorter oligonucleotides in urine (Table 5), consistent with mainly endonuclease-mediated metabolism. Moreover, the IP-HPLC provided baseline resolution for a majority of the metabolites, with nucleotide length of seven to 14 nucleotides (Fig. 8). In tissues analyzed by CGE, the same metabolites were detected, suggesting that

TABLE 4

Fraction of ISIS 301012 dose excreted (percentage) in urine as ISIS 301012 (parent drug) and its metabolites over the period of 0 to 24 h following intravenous and subcutaneous injection at selected doses compared across species

Parameter	Mouse		Rat[a]	Monkey		Human	
Route	s.c. Injection	s.c. Injection	i.v. Bolus	1-h i.v. Infusion	1-h i.v. Infusion	2-h i.v. Infusion	2-h i.v. Infusion
Dose	5 mg/kg	25 mg/kg	5 mg/kg	2 mg/kg	12 mg/kg	50 mg	200 mg
f_{ex}, ISIS 301012	1.05	22.2	NM	0.04	2.35	0.91	1.76
f_{ex}, metabolites	0	1.5	NM	0.22	0.54	0.47	1.54
f_{ex}, total	1.05	23.7	16	0.26	2.89	1.38	3.30

f_{ex}, fraction of administered dose excreted in urine; NM, not measured.

[a] Fraction (percentage) of total radiolabel dose excreted in urine.

Downloaded from dmd.aspetjournals.org at ASPET Journals on March 5, 2016

these metabolites are generated in tissues and subsequently excreted in urine.

Discussion

Plasma pharmacokinetics of the of 2′-MOE partially modified ISIS 301012 was similar in mice, rats, monkeys, and humans in that drug was cleared from plasma rapidly and distributed to tissues. This pharmacokinetic behavior has been observed for unmodified phosphorothioate oligodeoxynucleotides (first-generation oligodeoxynucleotides) as well as other 2′-MOE partially modified oligodeoxynucleotides of the same chemical class as ISIS 30102 but of different sequence (Geary et al., 1997a, 2003). After parenteral administration, plasma concentration-time profiles of ISIS 301012 are polyphasic, characterized by a rapid distribution phase (half-lives in hours), followed by at least one additional much slower elimination phase with half-lives from 5 to 31 days. The recent development of ultrasensitive hybridization ELISA methods have made it possible to characterize plasma concentrations up to 3 months after dose administration, enabling the determination of terminal plasma elimination half-lives (Yu et al., 2001c, 2002; Sewell et al., 2002; Geary et al., 2003). Most importantly, the plasma concentrations of ISIS 301012 observed in the terminal elimination phase represent ISIS 301012 that is in equilibrium with tissue(s) and thus provides a measure of tissue elimination rate (based on nonclinical experience with measured tissue elimination over time).

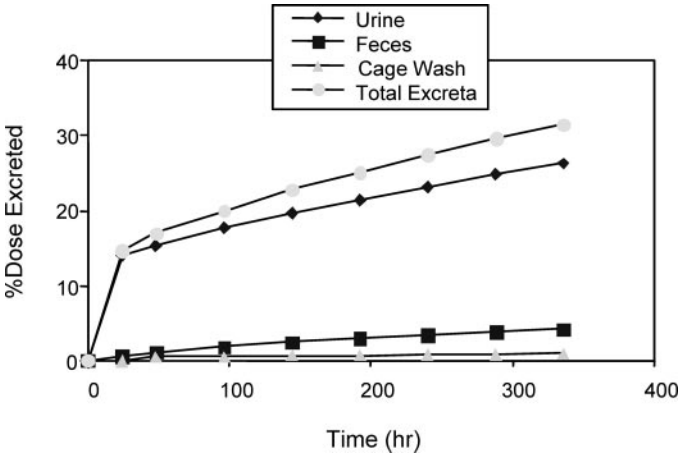

FIG. 7. Mass balance excretion of radiolabel residue associated with [^{3}H]ISIS 301012 over 14 days after single 5-mg/kg i.v. bolus injection in rats.

Allometric analysis of plasma pharmacokinetics for multiple ASOs from mouse to man confirm the predictability of the pharmacokinetics across species and the ability to extrapolate exposure directly on a milligram per kilogram basis (Geary et al., 1997a,b, 2003). These relationships are once again demonstrated with ISIS 301012 data, where plasma clearance and unbound intrinsic clearance scaled well across species using body weight.

The majority of drug was removed from plasma by distribution to tissues within the first 24 h after drug administration. The low abundance of the shortened metabolites in tissue is consistent with the long tissue elimination half-life of this compound and the short half-life of the metabolites. Relative to plasma distribution (half-life in minutes to hours), tissue elimination was slow (half-life in days). ISIS 301012 in tissue was cleared slowly over the course of weeks, and tissue half-lives are approximately 5-fold longer than for first-generation ASOs (Agrawal et al., 1995; Phillips et al., 1997; Geary et al., 2001c, 2003; Yu et al., 2001a, 2004). The slow clearance from tissues allowed for maintenance of tissue concentrations with relatively infrequent dosing. Nevertheless, care must be taken in the interpretation of the terminal elimination rate, since it is, by definition, a composite of multiple tissues with the slowest eliminating tissue ultimately dominating the composite plasma elimination rate. The observed organ-to-organ differences in ISIS 301012 clearance together with previously described differences in suborgan cellular elimination rates (Yu et al., 2001d), indicate that it is at least possible that the elimination rate described by the terminal plasma phase will overestimate the half-life

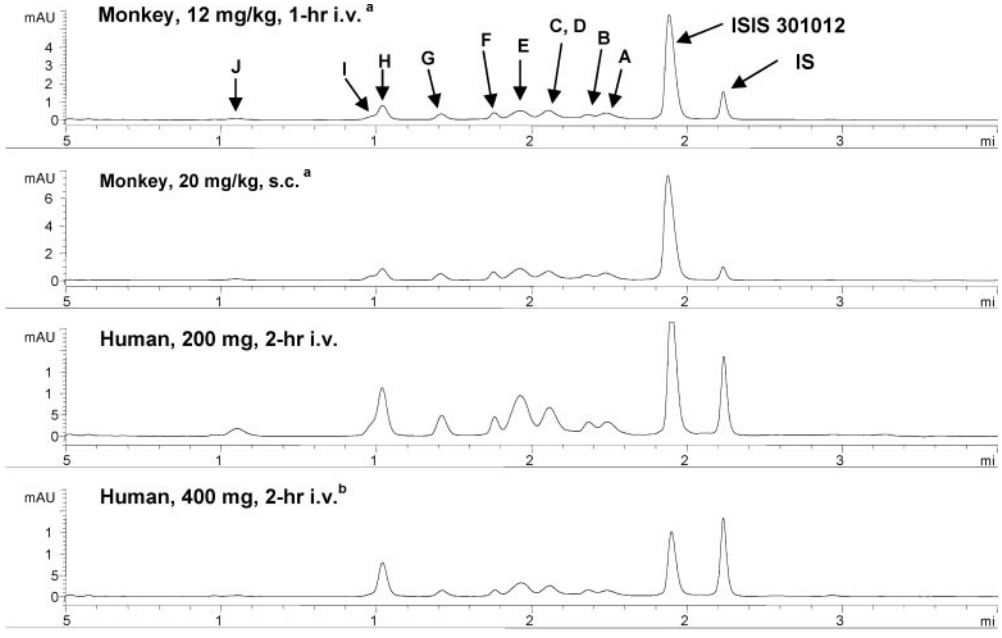

FIG. 8. Representative IP-HPLC chromatogram of urine samples collected at 0 to 24 h from monkeys and humans treated with ISIS 301012.

Refer to Table 3 for peak identifications.
[a] Sample was diluted 1:10 prior to extraction and analysis.
[b] Sample was diluted 1:5 prior to extraction and analysis.

Downloaded from dmd.aspetjournals.org at ASPET Journals on March 5, 2016

TABLE 5

Tabular summary of liquid chromatography-ES/MS results for monkey and human urine (0- to 24-h collection, monkey dose: 12 mg/kg; human dose: 400 mg)

Name[a]	Length	Sequence	Charge State	*m/z*	Molecular Mass Expected	Molecular Mass Observed	Δ MS
					Da		
ISIS 301012	20	GCCTCAGTCTGCTTCGCACC	−4	1793.1	7176.1	7176.4	0.3
A	14	GTCTGCTTCGCACC	−3	1616.8	4853.7	4853.1	−0.6
B	13	TCTGCTTCGCACC	−3	1501.6	4507.7	4508.4	0.7
C	11	TGCTTCGCACC	−3	1288.5	3868.6	3868.2	−0.4
D	10	P(S)-GCTTCGCACC	−3	1208.3	3628.5	3628.8	0.3
E	10	GCTTCGCACC	−3	1181.7	3548.6	3548.4	−0.2
F	10	GCCTCAGTCT	−3	1182.1	3549.6	3549.9	0.3
G	9	GCCTCAGTC	−3	1075.4	3229.5	3228.8	−0.7
H	8	GCCTCAGT	−3	968.9	2909.5	2910	0.5
I	8	TTCGCACC	−3	960.5	2883.5	2883.6	0.1
J	7	GCCTCAG	−2	1293.5	2589.5	2589	−0.5

[a] Refer to Fig. 10 for peak identifications.

at the target tissue and/or cell. Ultimately, a combination of clinical testing of multiple-dosing frequencies and careful pharmacokinetic/pharmacodynamic analysis should be used to fully characterize the optimal dosing frequency required to ensure continued pharmacological activity at the target.

Although distribution to tissues was the mechanism of plasma clearance, whole-body clearance is the result of slow metabolism by endo- and exonucleases in tissues, followed by urinary excretion of low-molecular weight oligonucleotide metabolites as well as ISIS 301012, and to a much lesser extent, fecal excretion of both ISIS 301012 and these metabolites. Ubiquitous endo- and exonucleases are known to metabolize oligonucleotides such as ISIS 301012. The endonuclease metabolism results in the formation of oligonucleotide fragments that are the substrates for additional metabolism by exonucleases. The resultant metabolites are shortened oligonucleotides of approximately eight to 12 nucleotides. The metabolites observed in urine are evidence that the earliest cleavage occurs in the 10-base 2′-deoxy gap, effectively splitting the oligomer in half. These data implicate endonuclease digestion as the initial cleavage event. These data are consistent with the nuclease resistance of 2′-MOE-modified nucleotides placed in the 3′- and 5′-terminal portions of ISIS 301012 (Zhang et al., 1995). There was a notable absence of metabolites ranging from 16 to 19 nucleotides, suggesting little to no exonuclease products that are often seen with unmodified phosphorothioate oligodeoxynucleotides (Temsamani et al., 1994; Cummins et al., 1996; Gaus et al., 1997). The similarity of the excretion metabolite pattern across species suggests similar enzymes are responsible for metabolic cleavage of oligonucleotides.

The pharmacokinetics of ISIS 301012 in human is predictable from the pharmacokinetics measured in monkey based on the similarities in plasma pharmacokinetics (C_{max}, AUC, and clearance) and plasma elimination half-life. Because the primary driver for plasma clearance is uptake by tissues, the similarities in the plasma kinetics suggest that there are similarities in distribution as well. Indeed, tissue distribution of ISIS 301012 was similar across species. Like unmodified predecessors, ISIS 301012 is rapidly distributed to tissues but with much longer tissue half-lives. These favorable pharmacokinetic properties for ISIS 301012 provide guidance for clinical development and seem to support infrequent and convenient dose administration.

Acknowledgments. We thank Dr. Art Levin for scientific discussion and critical review of the article. This article would not be possible without the administrative support provided by Robert Saunders, for which we are grateful.

References

Agrawal S, Temsamani J, Galbraith W, and Tang J (1995) Pharmacokinetics of antisense oligonucleotides. *Clin Pharmacokinet* **28:**7–16.

Altmann K-H, Dean NM, Fabbro D, Freier SM, Geiger T, Haner R, Husken D, Martin P, Monia BP, Muller M, et al. (1996) Second generation of antisense oligonucleotides: from nuclease resistance to biological efficacy in animals. *Chimia* **50:**168–176.

Boxenbaum H (1982) Interspecies scaling, allometry, physiological time, and the ground plan of pharmacokinetics. *J Pharmacokinet Biopharm* **10:**201–227.

Bradley JD, Crooke R, Kjems LL, Graham M, Leong R, Yu R, Paul D, and Wedel M (2005) Hypolipidemic effects of a novel inhibitor of human APO-B 100 in humans. *Diabetes* **54 (Suppl 1):**977-P.

Chi KN, Eisenhauer E, Fazli L, Jones EC, Goldenberg SL, Powers J, and Gleave ME (2005) A phase I pharmacokinetic and pharmacodynamic study of OGX-011, a 2′methoxyethyl antisense to clustering, in patients with localized prostate cancer. *J Natl Cancer Inst* **97:**1287–1296.

Cossum PA, Sasmor H, Dellinger D, Truong L, Cummins L, Owens SR, Markham PM, Shea JP, and Crooke ST (1993) Disposition of the 14C-labeled phosphorothioate oligonucleotide ISIS 2105 after intravenous administration to rats. *J Pharmacol Exp Ther* **267:**1181–1190.

Crooke RM, Graham MJ, Lemonidis KM, Whipple CP, Koo S, and Perera RJ (2005) An apolipoprotein B antisense oligonucleotide lowers LDL cholesterol in hyperlipidemic mice without causing hepatic steatosis. *J Lipid Res* **46:**872–884.

Cummins LL, Leeds J, Greig M, Griffey RH, Graham MJ, Crooke R, and Gaus HJ (1996) Capillary gel electrophoresis and mass spectrometry: powerful tools for the analysis of antisense oligonucleotides and their metabolites, in *XII International Roundtable, Nucleosides, Nucleotides and their Biological Applications*, p 72; 1996 Sept 15–19, La Jolla, CA.

Das HK, Leff T, and Breslow JL (1988) Cell type-specific expression of the human apoB gene is controlled by two *cis*-acting regulatory regions. *J Biol Chem* **263:**11452–11458.

Davidson NO and Shelness GS (2000) Apolipoprotein B: mRNA editing, lipoprotein assembly, and presecretory degradation. *Annu Rev Nutr* **20:**169–193.

Gaus HJ, Owens SR, Winniman M, Cooper S, and Cummins LL (1997) On-line HPLC electrospray mass spectrometry of phosphorothioate oligonucleotide metabolites. *Anal Chem* **69:**313–319.

Geary RS, Khatsenko O, Bunker K, Crooke R, Moore M, Burckin T, Truong L, Sasmor H, and Levin AA (2001a) Absolute bioavailability of 2′-*O*-(2-methoxyethyl)-modified antisense oligonucleotides following intraduodenal instillation in rats. *J Pharmacol Exp Ther* **296:**898–904.

Geary RS, Leeds JM, Fitchett J, Burckin T, Troung L, Spainhour C, Creek M, and Levin AA (1997a) Pharmacokinetics and metabolism in mice of a phosphorothioate oligonucleotide antisense inhibitor of C-raf-1 kinase expression. *Drug Metab Dispos* **25:**1272–1281.

Geary RS, Leeds JM, Henry SP, Monteith DK, and Levin AA (1997b) Antisense oligonucleotide inhibitors for the treatment of cancer: 1. Pharmacokinetic properties of phosphorothioate oligodeoxynucleotides. *Anticancer Drug Des* **12:**383–393.

Geary RS, Mathison B, Ushiro-Watanabe T, Savides MC, Henry SP, and Levin AA (2001b) Second generation antisense oligonucleotide pharmacokinetics and mass balance following intravenous administration in rats, in Society of Toxicology, p 343. Oxford University Press, San Francisco, CA.

Geary RS, Matson J, and Levin AA (1999) A nonradioisotope biomedical assay for intact oligonucleotide and its chain-shortened metabolites used for determination of exposure and elimination half-life of antisense drugs in tissue. *Anal Biochem* **274:**241–248.

Geary RS, Ushiro-Watanabe T, Truong L, Freier SM, Lesnik EA, Sioufi NB, Sasmor H, Manoharan M, and Levin AA (2001c) Pharmacokinetic properties of 2′-*O*-(2-methoxyethyl)-modified oligonucleotide analogs in rats. *J Pharmacol Exp Ther* **296:**890–897.

Geary RS, Yu RZ, Watanabe T, Henry SP, Hardee GE, Chappell A, Matson J, Sasmor H, Cummins L, and Levin AA (2003) Pharmacokinetics of a tumor necrosis factor-α phosphorothioate 2′-*O*-(2-methoxyethyl) modified antisense oligonucleotide: comparison across species. *Drug Metab Dispos* **31:**1419–1428.

Grindel JM, Musick TJ, Jiang Z, Roskey A, and Agrawal S (1998) Pharmacokinetics and metabolism of an oligodeoxynucleotide phosphorothioate (GEM91) in cynomolgus monkeys following intravenous infusion. *Antisense Nucleic Acid Drug Dev* **8:**43–52.

Henry SP, Geary RS, Yu R, and Levin AA (2001) Drug properties of second-generation antisense oligonucleotides: how do they measure up to their predecessors? *Curr Opin Investig Drugs* **2:**1444–1449.

Jones BA and Schreiber AD (2005) mRNA as a therapeutic target in lung disease. *Drug Design Rev-Online* **2:**361–372.

Kastelein JJP, Wedel MK, Baker BF, Su J, Bradley JD, Yu RZ, Chuang E, Graham MJ, and

Downloaded from dmd.aspetjournals.org at ASPET Journals on March 5, 2016

Crooke RM (2006) Potent reduction of apolipoprotein B and LDL cholesterol by an antisense inhibitor of apolipoprotein B. *Circulation* **114:**1729–1735.
Kjems L (2005) New targets for glycemic control protein-tyrosine-phosphatase-1B antisense inhibitor. *65th Annual Meeting of the American Diabetes Association*; 2005 Jun 10–14; San Diego, CA. American Diabetes Association, Alexandria, VA.
Leeds JM, Geary RS, Henry SP, Glover J, Shanahan W, Fitchett J, Burckin T, Truong L, and Levin AA (1997) Pharmacokinetic properties of phosphorothioate oligonucleotides. *Nucleosides Nucleotides* **16:**1689–1693.
Leeds JM, Graham MJ, Troung L, and Cummins LL (1996) Quantitation of phosphorothioate oligonucleotides in human plasma. *Anal Biochem* **235:**36–43.
Lima WF, Venkatraman M, and Crooke ST (1997) The influence of antisense oligonucleotide-induced RNA structure on E. coli RNase H1 activity. *J Biol Chem* **272:**18191–18199.
Manoharan M (1999) 2′-Carbohydrate modifications in antisense oligonucleotide therapy: importance of conformation, configuration and conjugation. *Biochim Biophys Acta* **1489:**117–130.
Marsh JB, Welty FK, Lichtenstein AH, Lamon-Fava S, and Schaefer EJ (2002) Apolipoprotein B metabolism in humans: studies with stable isotope-labeled amino acid precursors. *Atherosclerosis* **162:**227–244.
McKay RA, Miraglia LJ, Cummins LL, Owens SR, Sasmor H, and Dean NM (1999) Characterization of a potent and specific class of antisense oligonucleotide inhibitor of human protein kinase C-a expression. *J Biol Chem* **274:**1715–1722.
Phillips JA, Craig SJ, Bayley D, Christian RA, Geary RS, and Nicklin PL (1997) Pharmacokinetics, metabolism and elimination of a 20-mer phosphorothioate oligodeoxynucleotide (CGP 69846A) after intravenous and subcutaneous administration. *Biochem Pharmacol* **54:**657–668.
Sambrook J, Maniatis T, and Fritsche EF (1982) *Molecular Cloning: A Laboratory Manual*, Cold Spring Harbor Laboratory Press, Cold Spring Harbor, NY.
Sewell LK, Geary RS, Baker BF, Glover JM, Mant TGK, Yu RZ, Tami JA, and Dorr AF (2002) Phase I trial of ISIS 104838, a 2′-methoxyethyl modified antisense oligonucleotide targeting tumor necrosis factor-alpha. *J Pharmacol Exp Ther* **303:**1334–1343.
Temsamani J, Kubert M, Tang J, Padmapriya A, and Agrawal S (1994) Cellular uptake of oligodeoxynucleotide phosphorothioates and their analogs. *Antisense Res Dev* **4:**35–42.
Wagner RW (1994) Gene inhibition using antisense oligodeoxynucleotides. *Nature (Lond)* **372:**333–335.
Watanabe TA, Geary RS, and Levin AA (2006) Plasma protein binding of an antisense oligonucleotide targeting human ICAM-1 (ISIS 2302). *Oligonucleotides* **16:**169–180.
Wei N, Fiechtner J, Boyle D, Kavanaugh A, Delauter S, Rosengren S, Firestein GS, Tami J, Yu R, and Sewell L (2003) Synovial biomarker study of ISIS 104838, an antisense oligodeoxynucleotide targeting TNF-α, in rheumatoid arthritis. *67th Annual Meeting of the American College of Rheumatology*; 2003 Oct 23–28; Orlando, FL. American College of Rheumatology, Atlanta, GA.
Yu RZ, Baer B, Chappel A, Geary RS, Chueng E, and Levin AA (2002) Development of an ultrasensitive noncompetitive hybridization-ligation enzyme-linked immunosorbent assay for the determination of phosphorothioate oligodeoxynucleotide in plasma. *Anal Biochem* **304:**19–25.
Yu RZ, Geary RS, Leeds JM, Ushiro-Watanabe T, Moore M, Fitchett J, Matson J, Burckin T, Templin MV, and Levin AA (2001a) Comparison of pharmacokinetics and tissue disposition of an antisense phosphorothioate oligonucleotide targeting human Ha-ras mRNA in mouse and monkey. *J Pharm Sci* **90:**182–193.
Yu RZ, Geary RS, Monteith DK, Matson J, Truong L, Fitchett J, and Levin AA (2004) Tissue disposition of a 2′-*O*-(2-methoxy) ethyl modified antisense oligonucleotides in monkeys. *J Pharm Sci* **93:**48–59.
Yu RZ, Geary RS, Ushiro-Watanabe T, Levin AA, and Schoenfeld SL (2001b) Pharmacokinetic properties in humans, in *Antisense Drug Technology: Principles, Strategies, and Applications* (Crooke ST ed) pp 183–200, Marcel Dekker, Inc., New York.
Yu RZ, Matson J, and Geary RS (2001c) Terminal elimination rates for antisense oligonucleotides in plasma correlate with tissue clearance rates in mice and monkeys. *AAPS PharmSci* **3**.
Yu RZ, Zhang H, Geary RS, Graham M, Masarjian L, Lemonidis K, Crooke R, Dean NM, and Levin AA (2001d) Pharmacokinetics and pharmacodynamics of an antisense phosphorothioate oligonucleotide targeting Fas mRNA in mice. *J Pharmacol Exp Ther* **296:**388–395.
Zhang R, Lu Z, Zhao H, Zhang X, Diasio RB, Habus I, Jiang Z, Iyer RP, Yu D, and Agrawal S (1995) In vivo stability, disposition and metabolism of a "hybrid" oligonucleotide phosphorothioate in rats. *Biochem Pharmacol* **50:**545–556.

Address correspondence to: Dr. Rosie Z. Yu, Isis Pharmaceuticals, 1896 Rutherford Rd., Carlsbad, CA 92008. E-mail: ryu@isisph.com

Downloaded from dmd.aspetjournals.org at ASPET Journals on March 5, 2016